J Exp Biol Advance Online Articles. First posted online on 25 June 2015 as doi:10.1242/jeb.124826
Access the most recent version at http://jeb.biologists.org/lookup/doi/10.1242/jeb.124826

Scaling of cerebral blood perfusion in primates and marsupials

Roger S. Seymour*, Sophie E. Angove, Edward P. Snelling, Phillip Cassey

School of Biological Sciences, University of Adelaide, Adelaide, South Australia 5005, Australia

*Corresponding author: email: roger.seymour@adelaide.edu.au

Phone: +61 8 83135596

Summary statement: Brain blood flow rate increases with brain size and body size much faster in primates than in marsupial mammals, correlating with differences in cognitive ability.

Abstract

The evolution of primates involved increasing body size, brain size and presumably cognitive ability. Cognition is related to neural activity, metabolic rate and blood flow rate to the cerebral cortex. These parameters are difficult to quantify in living animals. This study shows that it is possible to determine the rate of cortical brain perfusion from the size of the internal carotid artery foramina in skulls of certain mammals, including haplorrhine primates and diprotodont marsupials. We quantify combined blood flow rate in both internal carotid arteries as a proxy of brain metabolism in 34 species of haplorrhine primates (0.116 – 145 kg body mass) and compare it to the same analysis for 19 species of diprotodont marsupials (0.014 – 46 kg). Brain volume is related to body mass by essentially the same exponent of 0.71 in both groups. Flow rate increases with haplorrhine brain volume to the 0.95 power, which is significantly higher than the exponent (0.75) expected for most organs according to "Kleiber's Law". By comparison, the exponent is 0.73 in marsupials. Thus the brain perfusion rate increases with body size and brain size much faster in primates than in marsupials. The trajectory of cerebral perfusion in primates is set by the phylogenetically older groups (New and Old World monkeys, lesser apes), and the phylogenetically younger groups (great apes, including humans) fall near the line, with the highest perfusion. This may be associated with disproportionate increases in cortical surface area and mental capacity in the highly social, larger primates.

Key words: allometry, brain metabolism, brain perfusion, cognition, primate evolution

Introduction

The evolution of primates involved an overall trend for increased body size, absolute brain size and relative brain size, although there are reversals in some primate clades (Montgomery et al., 2010). This overall size increase is presumably associated with increased brain metabolic rate and cognitive ability, leading to the great apes and humans. The human brain is an energy-expensive tissue (Aiello and Wheeler, 1995), and much current interest in primate brain evolution concerns how the high cost is compensated in primates compared to other mammals (Navarrete et al., 2011; Pontzer et al., 2014). Recent research shows that the number of neurons is directly proportional to brain size in primates (Herculano-Houzel, 2011c), and that the metabolic rate of the brain appears directly proportional to the number of neurons (Herculano-Houzel, 2011a). Therefore, within primates, brain metabolic rate is thought to be proportional to brain size, and the large human brain appears to be simply a scaled-up version of smaller primate brains (Herculano-Houzel, 2012). However, the relationship between brain metabolic rate and brain size in mammals may not follow direct proportionality. When brain metabolic rate in relation to brain mass was analysed with an allometric equation of the form, $Y = a\ X^b$, the exponent b was 0.82 when based on data from rats, dogs and humans (Wang et al., 2001). More recently, a meta-analysis of direct measurements of brain metabolic rate across ten species of mammal, from mouse to human, showed that it scales with brain volume to the 0.86 power, which is significantly higher than the commonly accepted exponent of 0.75 required by "Kleiber's Law" (Karbowski, 2007). Laboratory and domestic mammals occupy the small end of the brain size distribution (0.35 – 72 ml) in this analysis, and the primates are at the large end, with large brains (100 – 1389 ml). A larger sample of primate species over a greater range of body and brain size would not only provide a direct test of these important concepts, but also reflect on the evolution of brain metabolic rate and possibly cognitive ability among primates.

Brain metabolic rate is related to brain size and the intensity of neuronal and synaptic activity (Attwell and Laughlin, 2001). Compared to the entire body, the metabolic rate of the brain is high and is similar during mental activity and sleep (Armstrong, 1983), as well as during rest and moderate exercise (Hiura et al., 2014; Wilcox et al., 1970). On a tissue-mass-specific basis, brain metabolic rate in a resting mammal is about 2/3 of the rates of the most active organs (heart, liver, kidney) and more than ten times higher than that of the rest of the body (Wang et al., 2001). Continuous cranial blood flow is required because of the aerobic nature of the brain and its inability to store glucose or glycogen (Karbowski, 2011;

Weisbecker and Goswami, 2010). Blood flow rates in the internal carotid arteries are likely to indicate the levels of activity in the brain, because these vessels mainly supply the cerebrum (with minor supplies to the meninges, eyes and forehead scalp), while the vertebral arteries mainly supply the cerebellum in most mammals (Turnquist and Minugh-Purvis, 2012). Moreover, metabolic rate is much greater in a cerebral neuron than a cerebellar neuron (Herculano-Houzel, 2011c). Thus, blood flow rates in the internal carotid arteries of humans are considerably higher than in the vertebral arteries (Schöning et al., 1994). Direct measurements of carotid arterial blood flow rate and brain blood flow rate show a close correlation (van Bel et al., 1994).

Local cerebral blood flow in the internal carotid arteries is considered proportional to the metabolic rate of the cerebral cortex (Changizi, 2001; Hawkins et al., 1983; Lou et al., 1987; Turnquist and Minugh-Purvis, 2012). This is demonstrated quite clearly by similar allometric exponents for brain oxygen consumption rate, glucose utilization rate and cerebral perfusion rate in relation to brain volume, V_{br}. The rate of oxygen uptake by the whole brain of seven mammalian species scales with $V_{br}^{0.86}$ and the rate of glucose metabolism in ten species also scales with $V_{br}^{0.86}$ (Karbowski, 2007). The scaling of cortical blood flow rate and cortical brain volume in up to seven species of mammals varies with exponents between 0.81 and 0.87, depending on the particular part of the cortex, but the overall exponent is 0.84 (Karbowski, 2011). This indicates that there is good matching of brain metabolic rate and blood flow rate and confirms the notion that blood flow rate can indicate metabolic rate. The implication of proportionality between perfusion and metabolic rate is that O_2 extraction from the cerebral blood is constant. Thus it is not necessary to know arterial-venous O_2 contents, O_2–equilibrium curves, haemoglobin levels, transit times, intercapillary distances or other variables associated with O_2 delivery.

The metabolic rate of an organ influences the size of the supplying artery. Blood vessels undergo continuous remodelling throughout life in response to local haemodynamic forces, including blood pressure that affects vessel wall thickness, and blood flow rate that induces shear stress and causes changes in vessel lumen diameter (Lehoux et al., 2006). Vessel remodelling ensures that the energy needed for perfusion is minimised by maintaining basal levels of shear stress and producing energy-efficient laminar flow (Ward et al., 2000). Chronic and acute experimental changes in flow rates or blood pressure induce adaptive alteration in vessel geometry and normalize shear stress within narrow limits (Kamiya et al.,

1984; Kamiya and Togawa, 1980; Langille, 1999; Smiesko and Johnson, 1993; Tronc et al., 1996). Blood flow rate $\dot{Q}$ is related to shear stress τ, vessel radius r, and blood viscosity η according to the equation: $\dot{Q} = (\tau \pi r^3)/(4 \eta)$ (Lehoux and Tedgui, 2003). Shear stress is the viscous force exerted by the blood flowing along the walls of the vessel, and it is calculated as proportional to the maximum velocity at the axis of the vessel and inversely proportional to vessel radius, assuming a parabolic velocity distribution between the axis and the wall, where velocity is theoretically zero (Jeong and Rosenson, 2013). The vascular epithelium senses blood flow near the wall and induces a molecular mechanism of vascular remodelling that is well understood (Lu and Kassab, 2011). The biophysics involving arterial wall thickness is also well known. Larger arteries have thicker walls because wall cross-sectional tension is normalized according to the principle of Laplace that requires the wall thickness to increase in proportion to blood pressure and the radius of the vessel (Burton, 1965). Mean central arterial blood pressure is essentially invariant across species, except in mammals with long vertical distances between the heart and the head (White and Seymour, 2014), and blood viscosity is also invariant in mammals (Schmid-Schönbein et al., 1969). Therefore, measurements of external arterial dimensions can indicate the rate of blood flow within them. Where an artery passes through a foramen in a bone, the foramen size can be a gauge of arterial size, which is the key innovation that has allowed estimates of bone perfusion in living and extinct vertebrates (Allan et al., 2014; Seymour et al., 2012).

The present study estimates cerebral perfusion from the radius of the internal carotid foramen, measured in skulls of haplorrhine primates and diprotodont marsupials. This comparison was made for a number of reasons. The body sizes of haplorrhine primates and diprotodont marsupials overlap, with humans equivalent to large kangaroos. The blood supply to the forebrain of haplorrhine primates is mainly derived from the internal carotid arteries that service all of the tissues anterior to the hippocampus, while the vertebral arteries supply mainly the hindbrain, although there are connections between the two within the cerebral arterial circle (Circle of Willis) (Coceani and Gloor, 1966; Scremin, 2011). The same is true for diprotodonts; the internal carotid arteries supply the forebrain through discrete internal carotid foramina, while the vertebral arteries supply the hindbrain through the foramen magnum (Voris, 1928). Haplorhhine primates and marsupials have no additional arterial supplies to the forebrain (Gillilan, 1972). The analysis is not possible in most other groups of placental mammals, because the blood supply is derived from a complex of arteries, often involving retia and entering the skull through various foramina. Strepsirrhine

primates have much reduced internal carotid arteries (Schwartz and Tattersall, 1987), nevertheless, we include them for comparison in this study. Examples of other inappropriate groups unfortunately include cetaceans (Geisler and Luo, 1998; Viamonte et al., 1968 ; Vogl and Fisher, 1981), carnivores (Davis and Story, 1943; Gillilan, 1976) and artiodactyls (Diéguez et al., 1987; Gillilan, 1974). Rodents (Gillilan, 1974) and rabbits (Scremin et al., 1982) appear to have discrete internal carotid arteries, and deserve study, but most are relatively small animals.

The taxonomy of this paper considers that primates comprise two clades, the Suborder Strepsirrhini that includes the lemuriform primates and the Suborder Haplorrhini that includes the tarsiers and simians (= anthropoids). Haplorrhine primate evolution followed a path that gave rise to four clades in succession: the Platyrrhini (New World monkeys) and the Catarrhini, which include the Cercopithecidae (Old World monkeys), the Hylobatidae (lesser apes and gibbons) and the Hominidae (great apes) (Finstermeier et al., 2013; Perelman et al., 2011). We use phylogenetically informed regression analysis to test how the total internal carotid blood flow, which is the sum of flows in both arteries, increases with brain volume, while accounting for the statistical dependence of related species due to their common ancestral history.

Results

Brain volumes V_{br} for Strepsirrhini, Haplorrhini and Diprotodontia increase with body mass M_b with exponents of 0.69, 0.71 and 0.70, respectively (Fig. 1; Table 1). Relative brain volume (body-mass-specific) does not remove the allometric effect of body mass, but is a common measurement in the literature. To obtain it, the equations in Table 1 remain the same, except that the exponent changes to a negative value equal to the given exponent minus 1.0. ANCOVA showed no significant differences in exponent between any of the three groups ($P > 0.88$), but significant differences in elevation between all groups ($P < 0.001$). Thus, for 1 kg animals, V_{br} is 22.9 ml in Haplorrhini, 12.9 ml in Strepsirrhini and 5.3 ml in Diprotodontia.

The radius of the internal carotid foramen is our primary measurement for the three groups (Fig. 2; Table 1). ANCOVA shows that exponents of foramen radius r_{ICF} on V_{br} are all significantly different from each other ($P<0.05$). Johnson-Neyman (J-N) tests reveal no significant difference between the data for Diprotodontia and Haplorrhini within the range where V_{br} overlap, but Strepsirrhini are all significantly lower than the other two groups.

Total internal carotid blood flow rate ($\dot{Q}_{ICA}$), which is the sum of flows in both arteries, reflects the relationship of foramen size on V_{br}, but is not equivalent to it, because flow rate takes into account the scaling of shear stress with body mass (Fig. 3; Table 1). ANCOVA shows significant differences in exponents between the three groups ($P<0.05$). There is no significant difference in the data between Haplorrhini and Diprotodontia where the V_{br} overlaps, but the smallest three points for Diprotodontia are significantly higher than predicted from Haplorrhini (J-N test). All points for Strepsirrhini are significantly lower than any of the other groups (J-N test).

Total internal carotid blood flow rate increases with M_b in all three groups (Fig. 4; Table 1). ANCOVA shows that the exponents of $\dot{Q}_{ICA}$ on M_b are not significantly different between Haplorrhini and Diprotodontia ($P = 0.09$), but Haplorrhini have significantly higher elevation ($P <0.001$). The exponent for $\dot{Q}_{ICA}$ on M_b for Strepsirrhini is significantly higher than both the Haplorrhini and Diprotodontia, but the $\dot{Q}_{ICA}$ data are all significantly lower than those of all Haplorrhini, and all but the lemur *Propithecus diadema* are lower than Diprotodontia according to the J-N test.

Focussing on the Haplorrhini, a tight relationship exists between $\dot{Q}_{ICA}$ and V_{br}, with an exponent of 0.95 (Fig. 5). The 95% confidence interval for the exponent is 0.84 – 1.06. A trend towards larger brains with higher $\dot{Q}_{ICA}$ emerges throughout haplorrhine evolution, from the smaller brained New World monkeys to the large brained apes, including humans, with the highest $\dot{Q}_{ICA}$. Blood flow to the human brain is not exceptional and falls almost exactly on the regression line for haplorrhine primates in general.

For haplorrhine primates, the best supported phylogenetic model for explaining variability in $\log_{10}$-transformed $\dot{Q}_{ICA}$ includes V_{br} rather than M_b. This model was consistently the top-ranked model across all 1000 phylogenies (Table 2). The extent to which $\dot{Q}_{ICA}$ and V_{br} have evolved by Brownian motion (i.e., phylogenetic signal measured by Pagel's Lambda) was very strong among the species of Haplorrhini, indicating a high

correlation between brain perfusion derived from the internal carotid arteries and relatedness of species during primate evolution. Across all 1000 phylogenetic trees, the median maximum likelihood estimate of Pagel's Lambda in this model was 1.00. These results were also confirmed in the Diprodontia (Table 2).

Discussion

The scaling of brain volume V_{br} with body mass M_b in the two groups of primates and diprotodonts are parallel with nearly identical exponents of about 0.70 (Fig. 1; Table 1). However, at any given M_b, haplorrhine primates have brains about 4 times larger, and strepsirrhines 2.5 times larger, than diprotodont marsupials. The implications of these large differences in V_{br} are not clear, because the three groups show similarities in diet, locomotion and arboreal habitat, but it may be correlated with a relatively high degree of social interaction and cognitive ability in primates. Within primates, there is a correlation between brain size, innovation and social learning (Reader and Laland, 2002), which is not evident among marsupials.

Links between cognitive ability and brain volume or encephalization quotient have been difficult to sustain (Deaner et al., 2007; Henneberg, 1998; Herculano-Houzel, 2012), but cerebral metabolic rate and blood flow rate may be better, indeed more appropriate, correlates. It is clear that brain metabolism, inferred through internal carotid blood flow increases strongly with increasing brain size in haplorrhine primates with a relatively high scaling exponent, $V_{br}^{0.95}$, which is not significantly different from 1.0, but significantly greater than 0.75 (Fig. 5). The cerebral cortex of primates becomes increasingly convoluted in larger brains, and the surface area increases with an exponent much higher than 0.67 that is expected for geometric expansion with the same appearance (Chenn and Walsh, 2002; Luders et al., 2008; Radinsky, 1975). The anthropoid cerebral cortex is relatively thick and convoluted, with the degree of gyrification increasing significantly as brain volume increases (Zilles et al., 2013). In particular, the surface area and gyrification of the temporal lobes increases with a significantly greater exponent than predicted for geometric growth of the brain (Rilling and Seligman, 2002). Conversely, gyrification in diprotodont species does not

vary considerably with increasing brain size (Zilles et al., 2013), and this is reflected in the scaling of blood flow in diprotodont marsupials, which is proportional to a much lower exponent, $V_{br}^{0.73}$ (Fig. 3; Table 1). Although the exponents differ between haplorrhine primates and diprotodonts, the absolute perfusion rates through the internal carotid arteries are similar, where brain volume overlaps (Fig. 3). If perfusion rate is related to cognitive ability, we conclude that there is little difference between the smaller (phylogenetically older) primates and marsupials.

The large difference between the exponent of $\dot{Q}_{ICA}$ on brain volume between haplorrhine primates (0.95) and diprotodont marsupials (0.73) almost exactly straddles the exponent of 0.86 for brain metabolic rate (Karbowski, 2007) and 0.84 for brain perfusion (Karbowski, 2011). ANCOVA shows that neither 0.95 nor 0.73 are significantly different from 0.86, based on the samples and relationships considered here. One explanation for this result may be that the primates represented the high end, and non-primates the low end, of the range in Karbowski's analysis, which could result in an intermediate exponent. Indeed, there is further reason to believe that the scaling of brain metabolism of primates differs from non-primates. The scaling of neuronal density (number of neurons per milligram of brain) on brain mass gives a negative exponent of –0.37 in rodents, but –0.12 in primates (Herculano-Houzel, 2011a). Converting from neuronal density to total neuron number, the exponents in relation to brain mass become 0.63 and 0.88, respectively. Because metabolic rate is related to neuron number, it is clear that primates have a much steeper scaling than rodents.

The significant differences in exponents between primates and diprotodonts may be related to the scaling of neuron density in the two groups. In primates, neuron and non-neuron cell numbers increase linearly with brain volume, maintaining neuron and non-neuron cell densities and cell sizes (Herculano-Houzel, 2011b). Conversely, in diprotodonts, an increase in brain volume results in an increase in neuron size and a decrease in neuron density (Herculano-Houzel et al., 2006; Karbowski, 2007). Glucose and oxygen consumption per neuron appears independent of neuron size (Herculano-Houzel, 2011c; Karbowski, 2011), so the diprotodonts scale lower, with an exponent close to the expected 0.75 value of "Kleiber's Law". It would be informative to determine whether or not other non-primate groups scale similarly to diprotodonts.

The data for Strepsirrhini are significantly lower than both of the other groups, because the internal carotid arteries are not the main supply to the forebrain. The pattern of brain perfusion in lemurs is different from other primates (Schwartz and Tattersall, 1987). Dwarf lemurs and mouse lemurs (Cheirogaleidae) possess a highly reduced internal carotid artery and rely on the ascending pharyngeal artery. Sportive lemurs (Lepilemuridae) primarily rely on external carotid and vertebral arteries, and have reduced internal carotid, stapedial, and ascending pharyngeal arteries. Three other families of lemurs (Lemuridae, Indriidae, Daubentoniidae) rely on large stapedial arteries and reduced internal carotids. The carotid foramen is therefore a poor indicator of brain perfusion in strepsirrhine primates.

A perplexing feature of the data is that calculated brain perfusion in diprotodont marsupial brains is not significantly different from haplorrhine brains within the range of overlapping brain volume (Fig. 3). This is in stark contrast with measurements of lower cellular and neuronal densities of the South American marsupial, the short-tailed opossum *Monodelphis domestica*, and estimates that the energy consumption of the neocortex of marsupials is less than 10% of that in similarly-sized eutherians (Seelke et al., 2014). At this stage, we cannot provide a satisfactory explanation for why brain perfusion appears relatively high, particularly in the small diprotodonts, however it could relate to differences in O_2 extraction.

The evolution of primate brain perfusion

The observed allometric relationship between brain perfusion and brain volume in primates increased from the small-bodied, small-brained New World monkeys to the larger Old World monkeys, and finally to the great apes and humans (Fig. 5) (Martin, 2001). According to mitochondrial genomes, the Strepsirrhini (lemuriform primates) gave rise to the Haplorrhini (tarsiers and anthropoid Haplorrhini) about 66 – 69 Mya, the Platyrrhini (New World monkeys) split from the Catarrhini (Old World monkeys and apes) about 46 Mya, the Hominoidea (apes) arose about 32 Mya and the Hylobatidae (lesser apes and gibbons) split from the Hominidae (great apes) about 19 Mya (Finstermeier et al., 2013). Our phylogenetically-informed analysis reveals a higher than expected blood flow relative to brain size as these major primate groups evolved. This may reflect an increase in cognitive activity and relative intelligence in primates, and the evolutionary correlates behind this trajectory may involve social behaviour, pair-bonding, dietary changes, among others

(Dunbar and Shultz, 2007a; Dunbar and Shultz, 2007b). To facilitate the increasing brain size, an increase in energy intake or decrease in energy expenditure on other organ development may have occurred (Aiello and Wheeler, 1995). In more advanced Haplorrhini, including human and chimpanzee, a dietary change from herbivorous to omnivorous resulted in consumption of more energy-dense foods. This shift may have not only increased energy intake without the need to increase foraging time, but also decreased the energy needed for digestive organs (Herculano-Houzel, 2012; Parker, 1996). The invention of cooking, which essentially softens and pre-digests food outside the digestive cavity may have further reduced energy requirements of digestion, allowing for a reduction in the size of the gastrointestinal tract (Herculano-Houzel, 2012). Interestingly, $\dot{Q}_{\mathrm{ICA}}$ in humans is exactly as predicted from the other primates for a 1.2 kg brain, indicating that humans are not exceptional in primate evolution other than having a large brain relative to body size.

Critique of methods

It is possible to provide three independent validations of actual blood flow rate and carotid foramen size in humans, rats and mice, because sufficient data are available (Table 3). Here we arrive at internal carotid blood flow rate in two ways: first, by obtaining actual measured blood flow rates from the literature (L), and second, by calculating flow rate from foramen radius according to the methods of the present (P) study. The L/P ratios of $\dot{Q}_{\mathrm{ICA}}$ are 1.28 for humans, 1.00 for rats and 1.35 for mice. The L/P ratios of lumen radius are 1.09, 1.00 and 1.10, respectively. Given that the shear stress equation includes lumen radius to the third power, the agreement between measured and calculated flow rates is fairly good.

We calculate the rate of blood flow through the carotid foramen according to the shear stress equation, $\dot{Q} = (\tau\ \pi\ r^3)/(4\ \eta)$, in which flow is proportional to the radius cubed. This equation does not require knowledge of blood pressure or vessel length. The equation is less common among circulation physiologists than the Poiseuille-Hagen (P-H) equation, $\dot{Q} = (\Delta P\ \pi\ r^4)/(8\ L\ \eta)$, in which flow rate is proportional to the pressure decrease (ΔP) along the vessel and to r^4/L, where L is the length of the vessel. Not only is L difficult to measure for the internal carotid, but also ΔP must be extremely small and most likely never measured. In any case, if r and L scale with body size geometrically ($\propto M_{\mathrm{b}}^{0.33}$), r^3 and r^4/L are allometrically equivalent.

We assume that brain case volume scales similarly with brain volume and we include the volume of the cerebellum that is perfused largely by vertebral arteries. Although the volume of the cerebellum in relation to the entire brain increases slightly in larger primates, from approximately 9% in small monkeys to 13% in great apes (Rilling and Insel, 1998), the difference is negligible compared to other uncertainties in the study.

Conclusion

Because the metabolic rate of the brain is related to its blood supply, the sizes of the carotid foramina can be used as an index of brain metabolism and possibly cognitive ability. The evolutionary lineage of Haplorrhini shows a relatively steep progression of increasing brain perfusion, compared to the diprotodont marsupials. The trajectory of primate brain evolution appears to have been determined before the great apes arrived, but they sit near the line and humans on it. Although humans have a large brain in relation to their body mass, brain perfusion in them appears to be simply another step in primate evolution and unexceptional. Whether primates differ from mammals in general is not known, because we are unable to gauge brain perfusion in other groups with the technique of this study.

Our approach to inferring metabolic rates from blood flow and foramen size is not only expedient, but also permits measurements that are not otherwise practical. In the present case, direct determination of the metabolic rate of the brain is technically difficult. However, measuring the carotid foramen is relatively simple and can be used for both extant and extinct species. The sizes of the carotid foramen in fossil *Sahelanthropus, Australopithecus* and extinct *Homo* may reveal changes in blood flow to the brain that can indicate a trend towards higher order thinking. A separate analysis for hominids could determine if the advent of cooking did in fact result in an increase in brain volume, and a subsequent increase in carotid foramen area due to increased brain metabolism.

Materials and methods

Morphometric data, including brain case volume and carotid foramen radii, were collected from 34 species of simian primates (Suborder Haplorrhini), 7 species of prosimian primates (Suborder Strepsirrhini) and, for comparison, 19 species of diprotodont marsupials (Order Diprotodontia).

Braincase volume (V_{br}) was measured in dried and degreased skulls by filling them with either millet seed (skulls < 200 ml) or sorghum seed (> 200 ml). After sealing major foramina with cotton wool, skulls were filled to just below the opening of the foramen magnum, and were uniformly agitated to ensure similar packing characteristics. Seed was then poured into an appropriately sized graduated cylinder and agitated to determine volume. Brain case volume is a reliable estimate of brain mass, as brain has a density of 1.04 g ml^{-1} (Isler et al., 2008).

We identified the carotid foramina from published anatomical illustrations of primate skulls (Ankel-Simons, 2007) and marsupial skulls (Reig et al., 1987; Travouillon et al., 2014) (Fig. 6). For primates, we measured the external opening of the carotid canal, not the foramen lacerum, which in living humans is sealed by cartilage on the outside of the skull but opens on the inside to pass the internal carotid artery (Tauber et al., 1999).

The minimum diameter of the carotid foramen, below the flared surface, was measured with callipers directly from large skulls. For small skulls, calibrated digital photographs were taken with a camera (LC20, Olympus Soft Imaging Solutions GmbH, Münster, Germany) mounted on a dissecting microscope (SZ2-ILST, Olympus Corporation, Tokyo, Japan) and foramen area was measured with image analysis software (ImageJ, www.nih.gov) (Fig. 7). Minimum diameter or area was converted to radius, which was the primary measurement that led to calculation of blood flow rate $\dot{Q}$ (cm^3 s^{-1}) according to the shear stress equation: $\dot{Q} = (\tau \pi r^3)/(4 \eta)$. The equation is independent of blood pressure, and blood viscosity (η) is taken as a constant (0.04 dyne s cm^{-1}) in the large vessels of mammals (Schmid-Schönbein et al., 1969). The other two variables, vessel lumen radius (r; cm), and shear stress (τ; dynes cm^{-2}) were evaluated as follows.

Lumen radius(r)

The shear stress equation requires the radius of the lumen of the internal carotid artery, not the radius of the carotid foramen. The internal carotid artery is the only significant blood vessel to pass through the carotid foramen, and it largely fills it. There is a thin layer of fascia, a few small veins, and the sympathetic internal carotid nerve plexus that passes as tiny fibres around and within the vessel wall (Drake et al., 2015). The internal and external radii of the arterial wall almost certainly scale in parallel with one another owing to the effect of the principle of Laplace for cylinders in requiring wall thickness to be directly proportional to lumen radius if blood pressure is constant (Burton, 1965). In fact, arterial blood pressure is practically invariant over the body mass range of primates (White and Seymour, 2014). The ratio of wall thickness (including intima, media and adventitia) to lumen radius is 0.40 in human common carotid arteries (Skilton et al., 2011), 0.40 in dog internal carotid arteries (Orsi et al., 2006) and 0.36 in rat brain posterior communicating arteries (Gules et al 2002). Thus we use the conversion: ICA lumen radius = (carotid foramen radius/1.4).

Shear stress (τ)

Although it is widely assumed that the circulatory system is constructed to normalize shear stress at a constant level (between ca. 10 – 20 dynes cm^{-2}), regardless of the section of the arterial tree or the mass of the animal, it is now clear that shear stress in major arteries decreases in larger mammals. Based on aortic flow rates measured with magnetic resonance angiography in mice, rats and humans, the scaling exponent is –0.38 (Greve et al., 2006). On theoretical grounds, other analyses independently predict an exponent of –0.375 for shear stress scaling in mammalian aortas, but indicate that this value is not necessarily universal for all arteries (Weinberg and Ethier, 2007). We estimated the scaling of shear stress for the internal carotid artery from measured data from 70 kg humans (this study) and 375 g rats (Cai et al., 2012) using the shear stress equation and literature values. Blood flow rate in one internal carotid artery is taken as 3.83 cm^3 s^{-1} in humans (Boysen et al., 1970) and 0.028 cm^3 s^{-1} in rats [mean of four studies: (Nakao et al., 2001; Ohno et al., 1979; Sakurada et al., 1978; Takagi et al., 1987)]. ICA lumen radius is taken as 0.221 cm in humans [mean of three studies: (Kane et al., 1996; Krejza et al., 2006; Porsche et al., 2002)] and 0.0304 in rats (Cai et al., 2012). Blood viscosity is considered invariant at 0.04 dyne s cm^{-1} (Schmid-Schönbein et al., 1969). The human and rat data produce a power equation, $\tau = 167\ M_b^{-0.20}$, which we

use to calculate ICA flow rate in this study. The exponent is less negative than that for aortas, but is similar to that for the common carotid artery (–0.21) derived from four species of mammal (Weinberg and Ethier, 2007).

Statistics

Internal carotid artery blood flow rate was calculated from the mean foramen size and then doubled to obtain total cerebral perfusion rate, $\dot{Q}_{ICA}$. A common $\dot{Q}_{ICA}$ datum for each species was obtained as a mean from one to ten adult specimens. Adult body mass of each species was obtained from the literature. All data were analysed allometrically using the power equation $Y = a\,X^b$, where Y is the variable of interest, X is the body mass or brain volume of the animal, a is the scaling factor (elevation of the curve) and b is the scaling exponent. The exponent indicates the shape of the relationship: Y is proportional to X only if $b = 1.0$; if $1 > b > 0$, the arithmetic curve of Y on X increases with an ever-decreasing slope and the ratio of Y/X decreases; if $b > 1.0$, the arithmetic curve increases with an ever-increasing slope and the ratio of Y/X increases. The power equation is often $\log_{10}$-transformed to a linear one: $\log Y = \log a + (b \log X)$. In this case b is the slope of the line. Ordinary least squares regressions on log-transformed data, 95% confidence intervals of regression means and significant differences between orders were determined using analysis of covariance (ANCOVA) in GraphPad Prism 5 statistical software (GraphPad Software, La Jolla, CA, USA) (Zar, 1998). When ANCOVA revealed differences in the exponent b, a Johnson-Neyman (J-N) test was performed to determine the range of X values over which the individual data for Y are significantly different (White, 2003).

Phylogenetic generalised least square (PGLS) models were constructed to test the association between $\log_{10}$-transformed values of $\dot{Q}_{ICA}$, M_b, and V_{br} in the haplorrhine primates and diprodont marsupials separately. PGLS models were constructed using the 'pgls' function in the package 'caper' (Orme et al., 2011) in the R software environment for statistical computing and graphics R Core Team (RCoreTeam, 2013). The 'pgls' function incorporated the covariance between related taxa into the calculation of estimated coefficients from a generalized least squares model. The covariance matrix of the expected covariance between each pair of tips was calculated using the branch lengths of an estimated phylogeny.

Haplorrhine primate phylogenetic trees were constructed online (http://10ktrees.fas.harvard.edu/Primates/index.html) using the "10kTrees dated phylogeny

v.3" with the associated taxonomy from GenBank (Arnold et al., 2010). One thousand phylogenetic trees were constructed, and PGLS models were assessed using Akaike Information Criterion (AICc) corrected for small sample sizes (Burnham and Anderson, 2001). A single Diprodont phylogenetic tree was obtained from a species-level phylogenetic supertree of marsupials (Cardillo et al., 2004). No phylogenetic analysis was done on the Strepsirrhini as the number of species was insufficient. Phylogenetic signal in blood flow index was measured by Pagel's lambda (λ) (Pagel, 1999). Pagel's lambda indicates the strength of the phylogenetic relationship, where values lie between 0 and 1. Lambda values of or near 0 are indicative of phylogenetic independence and values of or near 1 indicate that the variable is related to evolutionary history (Kamilar and Cooper, 2013).

Acknowledgments

We appreciate the efforts of many anonymous referees that improved our paper, especially the primatologists who instructed us to reanalyse our results and communicate them more clearly. We thank Cath Kemper and David Stemmer of the South Australian Museum for access to the primate collection and facilities, Maciej Henneberg for providing advice on the evolution of primate brains and access to his collections, Chris Macgowan for kindly providing original data on internal carotid flow in mice, and Qiaohui Hu for help with collecting data and literature and for drawing Figure 6.

Competing interests

The authors declare no competing or financial interests.

Author contributions

R.S.S., S.E.A. and E.P.S. designed and performed research and wrote the paper; P.C. performed the phylogenetic analysis and helped write the paper.

Funding

The project was funded by the Australian Research Council Discovery Grant (DP-120102081) to R.S.S. P.C. is an ARC Future Fellow (FT0991420).

References

Aiello, L. C. and Wheeler, P. (1995). The expensive-tissue hypothesis: the brain and the digestive system in human and primate evolution. *Current Anthropology* **36**, 199-221.

Allan, G. H., Cassey, P., Snelling, E. P., Maloney, S. K. and Seymour, R. S. (2014). Blood flow for bone remodelling correlates with locomotion in living and extinct birds. *Journal of Expermental Biology* **217**, 2956-2962.

Amin-Hanjani, S., Du, X., Pandey, D. K., Thulborn, K. R. and Charbel, F. T. (2015). Effect of age and vascular anatomy on blood flow in major cerebral vessels. *Journal of Cerebral Blood Flow and Metabolism* **35**, 312-318.

Ankel-Simons, F. (2007). Primate anatomy: an introduction. Third edition. Amsterdam & Boston: Elsevier.

Armstrong, E. (1983). Relative brain size and metabolism in mammals. *Science* **220**, 1302-1304.

Arnold, C., Matthews, L. J. and Nunn, C. L. (2010). The 10kTrees website: a new online resource for primate phylogeny. *Evolutionary Anthropology: Issues, News, and Reviews* **19**, 114-118.

Attwell, D. and Laughlin, S. B. (2001). An energy budget for signaling in the grey matter of the brain. *Journal of Cerebral Blood Flow and Metabolism* **21**, 1133-1145.

Bailey, S. A., Zidell, R. H. and Perry, R. W. (2004). Relationships between organ weight and body/brain weight in the rat: What is the best analytical endpoint? *Toxicologic Pathology* **32**, 448-466.

Bentourkia, M., Bol, A., Ivanoiu, A., Labar, D., Sibomana, M., Coppens, A., Michel, C., Cosnard, G. and De Volder, A. G. (2000). Comparison of regional cerebral blood flow and glucose metabolism in the normal brain: effect of aging. *Journal of the Neurological Sciences* **181**, 19-28.

Boysen, G., Ladegaard-Pedersen, H. J., Valentin, N. and Engell, H. C. (1970). Cerebral blood flow and internal carotid artery flow during carotid surgery. *Stroke* **1**, 253-260.

Burnham, K. P. and Anderson, D. R. (2001). Kullback-Leibler information as a basis for strong inference in ecological studies. *Wildlife Research* **28**, 111-119.

Burton, A. C. (1965). Physiology and Biophysics of the Circulation. Chicago: Year Book Medical Publishers Incorporated.

Cai, J., Sun, Y. H., Yuan, F. L., Chen, L. J., He, C., Bao, Y. H., Chen, Z. Q., Lou, M. Q., Xia, W. L., Yang, G. Y. et al. (2012). A novel intravital method to evaluate cerebral vasospasm in rat models of subarachnoid hemorrhage: A study with synchrotron radiation angiography. *Plos One* **7**, e33366.

Cardillo, M., Bininda-Emonds, R. P., Boakes, E. and Purvis, A. (2004). A species-level phylogenetic supertree of marsupials. *Journal of Zoology* **264**, 11-31.

Changizi, M. A. (2001). Principles underlying mammalian neocortical scaling. *Biological Cybernetics* **84**, 207-215.

Chenn, A. and Walsh, C. A. (2002). Regulation of cerebral cortical size by control of cell cycle exit in neural precursors. *Science* **297**, 365-369.

Coceani, F. and Gloor, P. (1966). The distribution of the internal carotid circulation in the brain of the macaque monkey (*Macaca mulatta*). *Journal of Comparative Neurology* **128**, 419-429.

Davis, D. D. and Story, H. E. (1943). The carotid circulation in the domestic cat. *Zoological Series; Field Museum of Natural History* **28 Publication 527**, 5-47.

Deaner, R. O., Isler, K., Burkart, J. and van Schaik, C. (2007). Overall brain size, and not encephalization quotient, best predicts cognitive ability across non-human primates. *Brain, Behavior and Evolution* **70**, 115-124.

Diéguez, G., García, A. L., Conde, M. V., Gómez, B., Santamaría, L. and Lluch, S. (1987). *In vitro* studies of the carotid rete mirabile of Artiodactyla. *Microvascular Research* **33**, 143-154.

Drake, R. L., Vogl, A. W. and Mitchell, A. W. M. (2015). Gray's Anatomy for Students. Philadelphia, PA, USA: Churchill Livingstone Elsevier.

Dunbar, R. I. and Shultz, S. (2007a). Understanding primate brain evolution. *Philosophical Transactions of the Royal Society B: Biological Sciences* **362**, 649-658.

Dunbar, R. I. M. and Shultz, S. (2007b). Evolution in the social brain. *Science* **317**, 1344-1347.

Finstermeier, K., Zinner, D., Brameier, M., Meyer, M., Kreuz, E., Hofreiter, M. and Roos, C. (2013). A mitogenomic phylogeny of living primates. *Plos One* **8**, e69504.

Geisler, J. H. and Luo, Z. (1998). Relationships of Cetacea to terrestrial ungulates and the evolution of cranial vasculature in Cete. In *The Emergence of Whales*, (ed. J. G. M. Thewissen), pp. 163-212. New York: Springer Science+Business Media.

Gillilan, L. A. (1972). Blood supply to primitive mammalian brains. *Journal of Comparative Neurology* **145**, 209-&.

Gillilan, L. A. (1974). Blood supply to brains of ungulates with and without a rete mirabile caroticum. *Journal of Comparative Neurology* **153**, 275-290.

Gillilan, L. A. (1976). Extra- and intra-cranial blood supply to brains of dog and cat. *American Journal of Anatomy* **146**, 237-253.

Greve, J. M., Les, A. S., Tang, B. T., Blomme, M. T. D., Wilson, N. M., Dalman, R. L., Pelc, N. J. and Taylor, C. A. (2006). Allometric scaling of wall shear stress from mice to humans: quantification using cine phase-contrast MRI and computational fluid dynamics. *American Journal of Physiology. Heart and Circulatory Physiology* **291**, H1700-H1708.

Hasegawa, M., Kida, I. and Wada, H. (2010). A volumetric analysis of the brain and hippocampus of rats rendered perinatal hypothyroid. *Neuroscience Letters* **479**, 240-244.

Hawkins, R. A., Mans, A. M., Davis, D. W., Hibbard, L. S. and Lu, D. M. (1983). Glucose availability to individual cerebral structures is correlated to glucose metabolism. *Journal of Neurochemistry* **40**, 1013-1018.

Henneberg, M. (1998). Evolution of the human brain: is bigger better? *Clinical and Experimental Pharmacology and Physiology* **25**, 745-749.

Herculano-Houzel, S. (2011a). Brains matter, bodies maybe not: the case for examining neuron numbers irrespective of body size. *Annals of the New York Academy of Sciences* **1225**, 191-199.

Herculano-Houzel, S. (2011b). Not all brains are made the same: new views on brain scaling in evolution. *Brain, Behavior and Evolution* **78**, 22-36.

Herculano-Houzel, S. (2011c). Scaling of brain metabolism with a fixed energy budget per neuron: implications for neuronal activity, plasticity and evolution. *Plos One* **6**, e17514.

Herculano-Houzel, S. (2012). The remarkable, yet not extraordinary, human brain as a scaled-up primate brain and its associated cost. *Proceedings of the National Academy of Sciences of the United States of America* **109**, 10661-10668.

Herculano-Houzel, S., Mota, B. and Lent, R. (2006). Cellular scaling rules for rodent brains. *Proceedings of the National Academy of Sciences of the United States of America* **103**, 12138-12143.

Hiura, M., Nariai, T., Ishii, K., Sakata, M., Oda, K., Toyohara, J. and Ishiwata, K. (2014). Changes in cerebral blood flow during steady-state cycling exercise: a study using oxygen-15-labeled water with PET. *Journal of Cerebral Blood Flow and Metabolism* **34**, 389-396.

Isler, K., Christopher Kirk, E., Miller, J., Albrecht, G. A., Gelvin, B. R. and Martin, R. D. (2008). Endocranial volumes of primate species: scaling analyses using a comprehensive and reliable data set. *Journal of Human Evolution* **55**, 967-978.

Jeong, S. K. and Rosenson, R. S. (2013). Shear rate specific blood viscosity and shear stress of carotid artery duplex ultrasonography in patients with lacunar infarction. *BMC Neurology* **13**.

Kamilar, J. and Cooper, N. (2013). Phylogenetic signal in primate behaviour, ecology and life history. *Philosophical Transactions of the Royal Society Series B-Biological Sciences* **368**, 20120341.

Kamiya, A., Bukhari, R. and Togawa, T. (1984). Adaptive regulation of wall shear stress optimizing vascular tree function. *Bulletin of Mathematical Biology* **46**, 127-137.

Kamiya, A. and Togawa, T. (1980). Adaptive regulation of wall shear stress to flow change in the canine carotid artery. *American Journal of Physiology. Heart and Circulatory Physiology* **239**, H14-H21.

Kane, A. G., Dillon, W. P., Barkovich, A. J., Norman, D., Dowd, C. F. and Kane, T. T. (1996). Reduced caliber of the internal carotid artery: A normal finding with ipsilateral absence or hypoplasia of the A1 segment. *American Journal of Neuroradiology* **17**, 1295-1301.

Karbowski, J. (2007). Global and regional brain metabolic scaling and its functional consequences. *BMC Biology* **5**, 18.

Karbowski, J. (2011). Scaling of brain metabolism and blood flow in relation to capillary and neural scaling. *Plos One* **6**, e26709.

Krejza, J., Arkuszewski, M., Kasner, S. E., Weigele, J., Ustymowicz, A., Hurst, R. W., Cucchiara, B. L. and Messe, S. R. (2006). Carotid artery diameter in men and women and the relation to body and neck size. *Stroke* **37**, 1103-1105.

Langille, B. L. (1999). Fluid dynamics in vascular pathology: adaptations of the arterial wall to chronic changes in blood flow. *Journal of Vascular Surgery* **29**, 1106-1108.

Lehoux, S., Castier, Y. and Tedgui, A. (2006). Molecular mechanisms of the vascular responses to haemodynamic forces. *Journal of Internal Medicine* **259**, 381-392.

Lehoux, S. and Tedgui, A. (2003). Cellular mechanics and gene expression in blood vessels. *Journal of biomechanics* **36**, 631-643.

Lou, H. C., Edvinsson, L. and MacKenzie, E. T. (1987). The concept of coupling blood flow to brain function: revision required? *Annals of Neurology* **22**, 289-297.

Lu, D. S. and Kassab, G. S. (2011). Role of shear stress and stretch in vascular mechanobiology. *Journal of The Royal Society Interface* **8**, 1379-1385.

Luders, E., Narr, K. L., Bilder, R. M., Szeszko, P. R., Gurbani, M. N., Hamilton, L., Toga, A. W. and Gaser, C. (2008). Mapping the relationship between cortical convolution and intelligence: effects of gender. *Cerebral Cortex* **18**, 2019-2026.

Macgowan, C. K., Stoops, S. J., Zhou, Y.-Q., Cahill, L. S. and Sled, J. G. (2015). Evaluation of cerebrovascular impedance and wave reflection in mouse by ultrasound. *Journal of Cerebral Blood Flow and Metabolism* **35**, 521-526.

Martin, R. D. (2001). Evolution of Primates. In *International Encyclopedia of the Social and Behavioral Sciences*, eds. N. Smelser and P. Baltes), pp. 12032-12038. Oxford: Pergamon.

Montgomery, S., Capellini, I., Barton, R. and Mundy, N. (2010). Reconstructing the ups and downs of primate brain evolution: implications for adaptive hypotheses and *Homo floresiensis*. *BMC Biology* **8**, 9.

Nakao, Y., Itoh, Y., Kuang, T.-Y., Cook, M., Jehle, J. and Sokoloff, L. (2001). Effects of anesthesia on functional activation of cerebral blood flow and metabolism. *Proceedings of the National Academy of Sciences of the United States of America* **98**, 7593–7598.

Navarrete, A., van Schaik, C. P. and Isler, K. (2011). Energetics and the evolution of human brain size. *Nature* **480**, 91-93.

Ohno, K., Pettigrew, K. D. and Rapoport, S. I. (1979). Local cerebral blood flow in the conscious rat as measured with ^{14}C-antipyrine, ^{14}C-iodoantipyrine and ^{3}H-nicotine. *Stroke* **10**, 62-67.

Orme, D., Freckleton, R., Thomas, G., Petzoldt, T., Fritz, S. and Isaac, N. (2011). Caper: Comparative Analyses of Phylogenetics and Evolution in R. In *R package version 0.4*.

Orsi, A. M., Domeniconi, R. F., Artoni, S. M. B. and Filho, J. G. (2006). Carotid arteries in the dog: Structure and histophysiology. *International Journal of Morphology* **24**, 239-244.

Pagel, M. (1999). Inferring the historical patterns of biological evolution. *Nature* **401**, 877-884.

Parker, S. T. (1996). Using cladistic analysis of comparative data to reconstruct the evolution of cognitive development in hominids. In *Phylogenies and the Comparative Method in Animal Behavior*, (ed. E. P. Martins), pp. 433-448. Oxford: Oxford University Press.

Perelman, P., Johnson, W. E., Roos, C., Seuánez, H. N., Horvath, J. E., Moreira, M. A. M., Kessing, B., Pontius, J., Roelke, M., Rumpler, Y. et al. (2011). A molecular phylogeny of living primates. *PLoS Genetics* **7**, e1001342.

Pontzer, H., Raichlen, D. A., Gordon, A. D., Schroepfer-Walker, K. K., Hare, B., O'Neill, M. C., Muldoon, K. M., Dunsworth, H. M., Wood, B. M., Isler, K. et al. (2014). Primate energy expenditure and life history. *Proceedings of the National Academy of Sciences of the United States of America* **111**, 1433-1437.

Porsche, C., Walker, L., Mendelow, A. D. and Birchall, D. (2002). Assessment of vessel wall thickness in carotid atherosclerosis using spiral CT angiography. *European Journal of Vascular and Endovascular Surgery* **23**, 437-440.

Radinsky, L. (1975). Primate brain evolution. *American Scientist* **63**, 656-663.

RCoreTeam. (2013). R: A language and environment for statistical computing. Vienna, Austria: R Foundation for Statistical Computing.

Reader, S. M. and Laland, K. N. (2002). Social intelligence, innovation, and enhanced brain size in primates. *Proceedings of the National Academy of Sciences of the United States of America* **99**, 4436-4441.

Reig, O. A., Kirsch, J. A. W. and Marshall, L. G. (1987). Systematic relationships of the living and Neocenozoic American 'opossum-like' marsupials (suborder Didelphimorphia), with comments on the classification of these and of the Cretaceous and Paleogene New World and European metatherians. In *Possums and opossums: studies in evolution*, (ed. M. Archer). Chipping Norton, N.S.W. : Surrey Beatty & Sons.

Rilling, J. K. and Insel, T. R. (1998). Evolution of the cerebellum in primates: differences in relative volume among monkeys, apes and humans. *Brain, Behavior and Evolution* **52**, 308-314.

Rilling, J. K. and Seligman, R. A. (2002). A quantitative morphometric comparative analysis of the primate temporal lobe. *Journal of Human Evolution* **42**, 505-533.

Sakurada, O., Kennedy, C., Jehle, J., Brown, J. D., Carbin, G. L. and Sokoloff, L. (1978). Measurement of local cerebral blood flow with iodo[^{14}C]antipyrine. *American Journal of Physiology* **234**, H59-H66.

Sato, T., Kawada, T., Miyano, H., Shishido, T., Inagaki, M., Yoshimura, R., Tatewaki, T., Sugimachi, M., Alexander, J. J. and Sunagawa, K. (1999). New simple methods for isolating baroreceptor regions of carotid sinus and aortic depressor nerves in rats. *American Journal of Physiology* **276 (Heart and Circulation Physiology 45)**, H326-H332.

Schmid-Schönbein, H., Wells, R. and Goldstone, J. (1969). Influence of deformability of human red cells upon blood viscosity. *Circulation Research* **25**, 131-143.

Schöning, M., Walter, J. and Scheel, P. (1994). Estimation of cerebral blood flow through color duplex sonography of the carotid and vertebral arteries in healthy adults. *Stroke* **25**, 17-22.

Schwartz, J. H. and Tattersall, I. (1987). Tarsiers, adapids and the integrity of Strepsirhini. *Journal of Human Evolution* **16**, 23-40.

Scremin, O. U. (2011). Cerebral vascular system. In *The Human Nervous system*, eds. J. Mai and G. Paxinos), pp. 1325-1348: Academic Press.

Scremin, O. U., Sonnenschein, R. R. and Rubinsstein, E. H. (1982). Cerebrovascular anatomy and blood flow measurements in the rabbit. *Journal of Cerebral Blood Flow and Metabolism* **2**, 55-66.

Seelke, A. M. H., Dooley, J. C. and Krubitzer, L. A. (2014). The cellular composition of the marsupial neocortex. *Journal of Comparative Neurology* **522**, 2286-2298.

Seymour, R. S., Smith, S. L., White, C. R., Henderson, D. M. and Schwarz-Wings, D. (2012). Blood flow to long bones indicates activity metabolism in mammals, reptiles and dinosaurs. *Proceedings of the Royal Society of London. Series B: Biological Sciences* **279**, 451-456.

Skilton, M. R., Boussel, L., Bonnet, F., Bernard, S., Douek, P. C., Moulin, P. and Serusclat, A. (2011). Carotid intima-media and adventitial thickening: Comparison of new and established ultrasound and magnetic resonance imaging techniques. *Atherosclerosis* **215**, 405-410.

Smiesko, V. and Johnson, P. C. (1993). The arterial lumen is controlled by flow-related shear stress. *News in Physiological Sciences* **8**, 34-38.

Tajima, A., Hans, F. J., Livingstone, D., Wei, L., Finnegan, W., Demaro, J. and Fenstermacher, J. (1993). Smaller local brain volumes and cerebral atrophy in spontaneously hypertensive rats. *Hypertension* **21**, 105-111.

Takagi, S., Ehara, K. and Finn, R. D. (1987). Water extraction fraction and permeability--Surface product after intravenous injection in rats. *Stroke* **18**, 177-183.

Tauber, M., Van Loveren, H. R., Jallo, G., Romano, A. and Keller, J. T. (1999). The enigmatic foramen lacerum. *Neurosurgery (Baltimore)* **44**, 386-393.

Travouillon, K. J., Cooke, B. N., Archer, M. and Hand, S. J. (2014). Revision of basal macropodids from the Riversleigh World Heritage Area with descriptions of new material of *Ganguroo bilamina* Cooke, 1997 and a new species. *Palaeontologia Electronica* **17**, 1.20A.

Tronc, F., Wassef, M., Esposito, B., Henrion, D., Glagov, S. and Tedgui, A. (1996). Role of NO in flow-induced remodeling of the rabbit common carotid artery. *Arteriosclerosis Thrombosis and Vascular Biology* **16**, 1256-1262.

Turnquist, J. E. and Minugh-Purvis, N. (2012). Functional Morphology. In *Nonhuman Primates in Biomedical Research (Second Edition)*, pp. 87-129. Boston: Academic Press.

van Bel, F., Roman, C., Klautz, R. J. M., Teitel, D. F. and Rudolph, A. M. (1994). Relationship between brain blood flow and carotid arterial flow in the sheep fetus. *Pediatric Research* **35**, 329-333.

Viamonte, M., Morgane, P. J., Galliano, R. E., Nagel, E. L. and McFarland, W. L. (1968). Angiography in the living dolphin and observations on blood supply to the brain. *American Journal of Physiology* **214**, 1225-1249.

Vogl, A. W. and Fisher, H. D. (1981). The internal carotid artery does not directly supply the brain in the Monodontidae (Order Cetacea). *Journal of Morphology* **170**, 207-214.

Voris, H. C. (1928). The arterial supply of the brain and spinal cord of the virginian opossum. (*Didelphis virginiana*). *Journal of Comparative Neurology* **44**, 403-423.

Wang, Z. M., O'Connor, T. P., Heshka, S. and Heymsfield, S. B. (2001). The reconstruction of Kleiber's law at the organ-tissue level. *Journal of Nutrition* **131**, 2967-2970.

Ward, M. R., Pasterkamp, G., Yeung, A. C. and Borst, C. (2000). Arterial remodeling: mechanisms and clinical implications. *Circulation* **102**, 1186-1191.

Weinberg, P. D. and Ethier, C. R. (2007). Twenty-fold difference in hemodynamic wall shear stress between murine and human aortas. *Journal of Biomechanics* **40**, 1594-1598.

Weisbecker, V. and Goswami, A. (2010). Brain size, life history, and metabolism at the marsupial/placental dichotomy. *Proceedings of the National Academy of Sciences* **107**, 16216-16221.

White, C. R. (2003). Allometric analysis beyond heterogeneous regression slopes: use of the Johnson-Neyman technique in comparative biology. *Physiological and Biochemical Zoology* **76**, 135-140.

White, C. R. and Seymour, R. S. (2014). The role of gravity in the evolution of mammalian blood pressure. *Evolution* **68**, 901-908.

Wilcox, B., Coulter, N., Rackley, C. and Croom, R. (1970). The effect of changing heart rate on blood flow, power dissipation, and resistance in the common carotid artery of man. *Annals of Surgery* **171**, 24-30.

Zar, J. H. (1998). Biostatistical Analysis. Englewood Cliffs, New Jersey: Prentice Hall.

Zilles, K., Palomero-Gallagher, N. and Amunts, K. (2013). Development of cortical folding during evolution and ontogeny. *Trends in Neurosciences* **36**, 275-284.

Tables

Table 1. Allometric equations of the form $Y = aX^b$, relating body mass (M_b), brain volume (V_{br}), total flow through both internal carotid arteries ($\dot{Q}_{ICA\times2}$) and internal carotid foramen radius (r_{ICF}) in two groups of primates (Strepsirrhini and Haplorrhini) and one group of marsupials (Diprotodontia). Ordinary least square regression equations are given with 95% confidence intervals for the exponent, coefficients of determination (r^2) and significant differences between the three groups according to ANCOVA. Exponents (*b*) of the allometric equations are significantly different ($P < 0.05$) if the letters A, B or C differ. If exponents are not different, then the elevation (*a*) is significantly different if the letters are different.

Independent	Dependent	Clade	Power equation	r^2	*b*	*a*
M_b (g)	V_{br} (ml)	Strepsirrhini	$1.04\times10^{-1}M_b^{0.69\pm0.10}$	0.99	A	A
		Haplorrhini	$1.73\times10^{-1}M_b^{0.71\pm0.09}$	0.89	A	B
		Diprotodontia	$4.19\times10^{-2}M_b^{0.70\pm0.06}$	0.98	A	C
M_b (g)	$\dot{Q}_{ICA}$ ($cm^3\ s^{-1}$)	Strepsirrhini	$5.73\times10^{-6}M_b^{1.07\pm0.76}$	0.72	A	
		Haplorrhini	$2.02\times10^{-3}M_b^{0.65\pm0.13}$	0.76	B	A
		Diprotodontia	$1.73\times10^{-3}M_b^{0.51\pm0.10}$	0.88	B	B
V_{br} (ml)	$\dot{Q}_{ICA}$ ($cm^3\ s^{-1}$)	Strepsirrhini	$1.90\times10^{-4}V_{br}^{1.56\pm1.06}$	0.74	A	
		Haplorrhini	$8.82\times10^{-3}V_{br}^{0.95\pm0.11}$	0.91	B	
		Diprotodontia	$1.71\times10^{-2}V_{br}^{0.73\pm0.11}$	0.92	C	
V_{br} (ml)	r_{ICF} (cm)	Strepsirrhini	$5.36\times10^{-3}V_{br}^{0.62\pm0.36}$	0.80	A	
		Haplorrhini	$1.91\times10^{-2}V_{br}^{0.40\pm0.04}$	0.95	B	
		Diprotodontia	$2.61\times10^{-2}V_{br}^{0.34\pm0.04}$	0.95	C	

Table 2. Model support (Akaike's information criterion; median AICc [1st and 99th percentiles]) for phylogenetic generalised least square models of total internal carotid blood flow rate ($Log_{10}(cm^3\ s^{-1})$; both arteries) in haplorrhine primates (34 species; 1000 phylogenetic hypotheses), and diprotodont marsupials (19 species; 1 phylogenetic hypothesis). Predictor variables (median estimate [1st and 99th percentiles] or [standard error]) are provided for the two models of adult body mass ($Log_{10}(g)$) and braincase volume ($Log_{10}(mL)$. Model ranks (and [no. of models]) and median relative model weights are also provided.

Intercept	Adult body mass $Log_{10}(g)$	Braincase volume $Log_{10}(ml)$	ΔAICc	Relative model weight	Model rank
Haplorrhine primates (34 species)					
-2.04 [-2.04, -2.05]		0.94 [0.94, 0.95]	0.00	1.00	1st [1000]
-2.68 [-2.67, -2.70]	0.64 [0.64, 0.65]		33.79 [32.97, 34.52]	0.00	2nd [1000]
Diprotodont marsupials (19 species)					
-1.77 [0.07]		0.73 [0.05]	0.00	0.967	1st
-2.77 [0.16]	0.51 [0.04]		6.75	0.033	2nd

Table 3. Measured and calculated cardiovascular variables relative to blood flow through the internal carotid arteries of humans and rats. Values are obtained from the literature (L) and the present study (P).

		Human		Rat		Mouse	
Variable	Unit		Ref.		Ref.		Ref.
Directly measured							
Body mass	g	70,000	1	375	9	26	13
Brain volume	ml	1186	1	1.96	10	0.35	8
Brain mass	g	1233	2	1.22	2	0.36	2
Cortical flow ($\dot{Q}_{ICA\ (L)}$)	$cm^3\ s^{-1}$	9.61	3	0.056	11	0.026	13
IC foramen radius ($r_{ICF\ (P)}$)	cm	0.307	1	0.040	12	0.025	14
Scaled variables							
Shear stress	$dyne\ cm^{-2}$	18.1	4	51.3	4	87.3	4
Blood viscosity	$dyne\ s\ cm^{-1}$	0.04	5	0.04	5	0.04	5
ICA wall:lumen radius		0.40	6	0.40	6	0.40	6
Calculated values							
ICA lumen radius ($r_{ICA\ (L)}$)	cm	0.24	7	0.030	7	0.020	7
ICA lumen radius ($r_{ICA\ (P)}$)	cm	0.22	6	0.030	9	0.018	14
Ratio ($r_{ICA\ (L)}$):($r_{ICA\ (P)}$)		1.09		1.00		1.10	
ICA wall thickness	cm	0.09	6	0.010	6	0.007	6
Cortical flow ($\dot{Q}_{ICA\ (P)}$)	$cm^3\ s^{-1}$	7.51	7	0.057	7	0.019	7
Ratio ($\dot{Q}_{ICA\ (L)}$):($\dot{Q}_{ICA\ (P)}$)		1.28		1.00		1.35	

References: 1. Present study; 2. Assumes brain density = 1.04 g ml^{-1} (Isler et al., 2008); 3. Mean of four studies (Amin-Hanjani et al., 2015; Bentourkia et al., 2000; Boysen et al., 1970; Hiura et al., 2014); 4. Calculated according to scaling body mass (see text); 5. (Schmid-Schönbein et al., 1969); 6. Ratio of wall thickness/lumen radius = 0.4; foramen radius = lumen radius * 1.4 (Orsi et al., 2006; Skilton et al., 2011); 7. Calculated from shear stress equation; 8. (Karbowski, 2007); 9. (Cai et al., 2012); 10. Mean of four studies (Bailey et al., 2004; Hasegawa et al., 2010; Karbowski, 2007; Tajima et al., 1993); 11. Mean of four studies (Nakao et al., 2001; Ohno et al., 1979; Sakurada et al., 1978; Takagi et al., 1987); 12. (Sato et al., 1999); 13. (Macgowan et al., 2015); 14. Christopher Macgowan (personal communication). ICA lumen radius from three mice. Foramen radius calculated from ICA lumen radius × 1.4 (note 6).

Figures

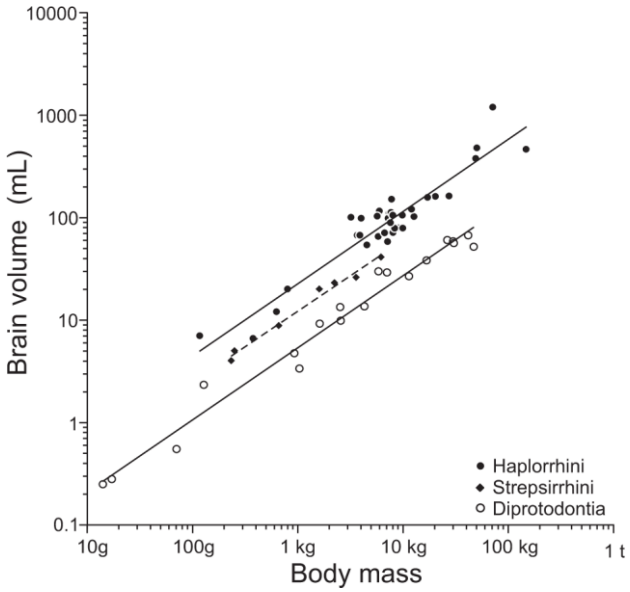

Figure 1. Relationship between brain volume and body mass. Data represent 34 species of Haplorrhini, seven species of Strepsirrhini and 19 species of diprotodont marsupials on log-log axes. See Table 1 for equations and statistics for the regression lines.

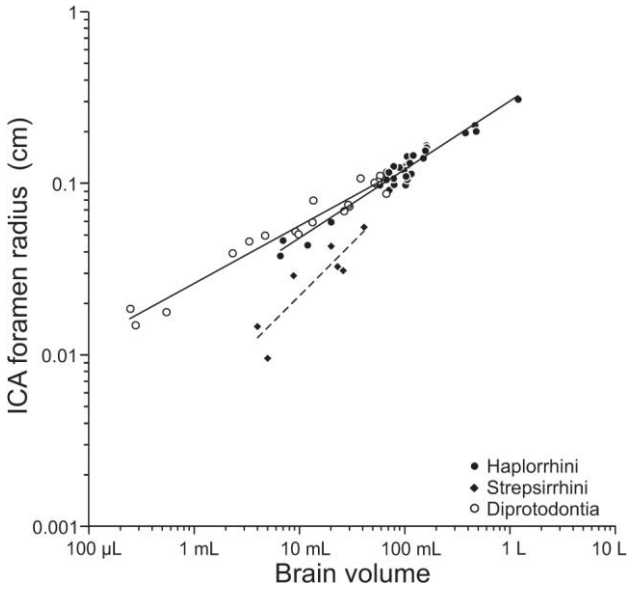

Figure 2. Relationship between internal carotid artery foramen radius and brain volume. See Table 1 for equations and statistics.

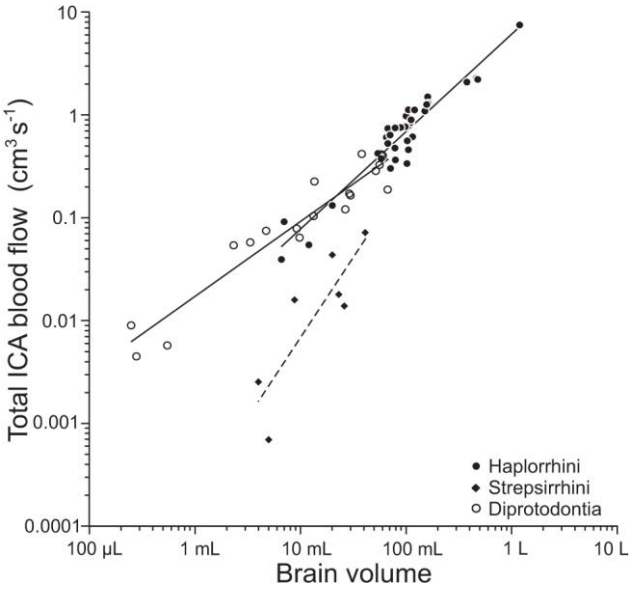

Figure 3. Relationship between total internal carotid blood flow rate (both arteries) and brain volume. See Table 1 for equations and statistics.

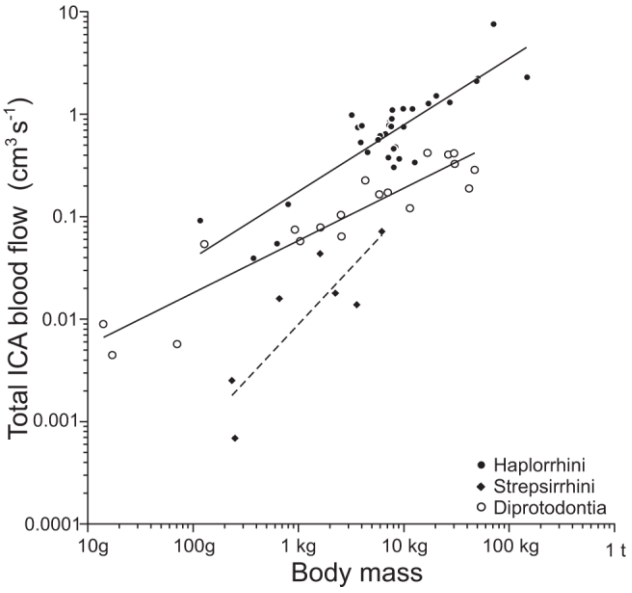

Figure 4. Relationship between total internal carotid blood flow rate (both arteries) and body mass. See Table 1 for equations and statistics.

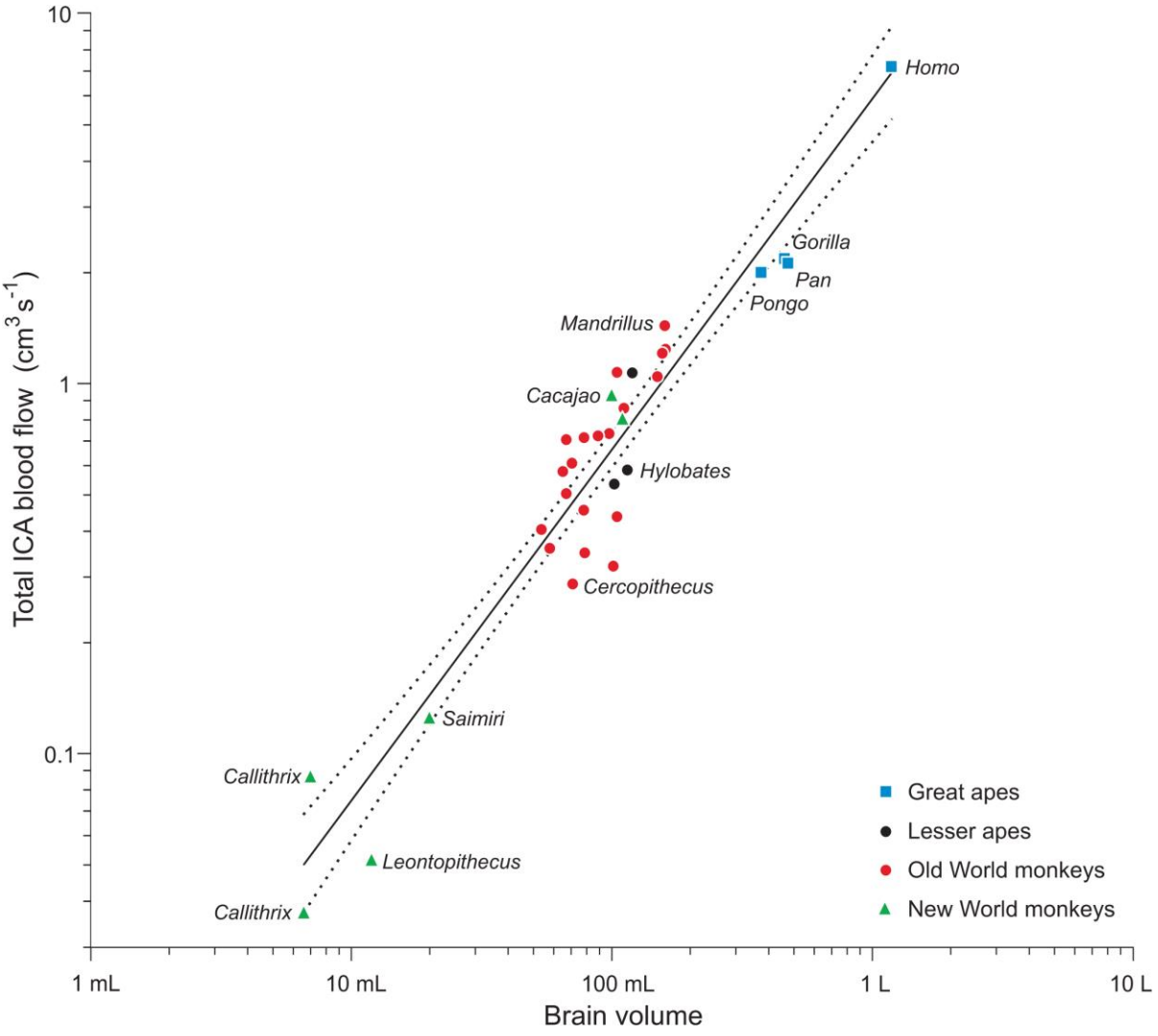

Figure 5. Relationship between total internal carotid blood flow rate (both arteries) and brain volume for Haplorrhini on log-log axes. Symbols represent the Family Hominidae (great apes), Family Hylobatidae (lesser apes), Superfamily Cercopithecidae (Old World monkeys), and Parvorder Platyrrhini (New World monkeys). Regression line and 95% confidence belts for the regression mean are shown. Selected genera are indicated. See the Supplementary Material for the full list of species.

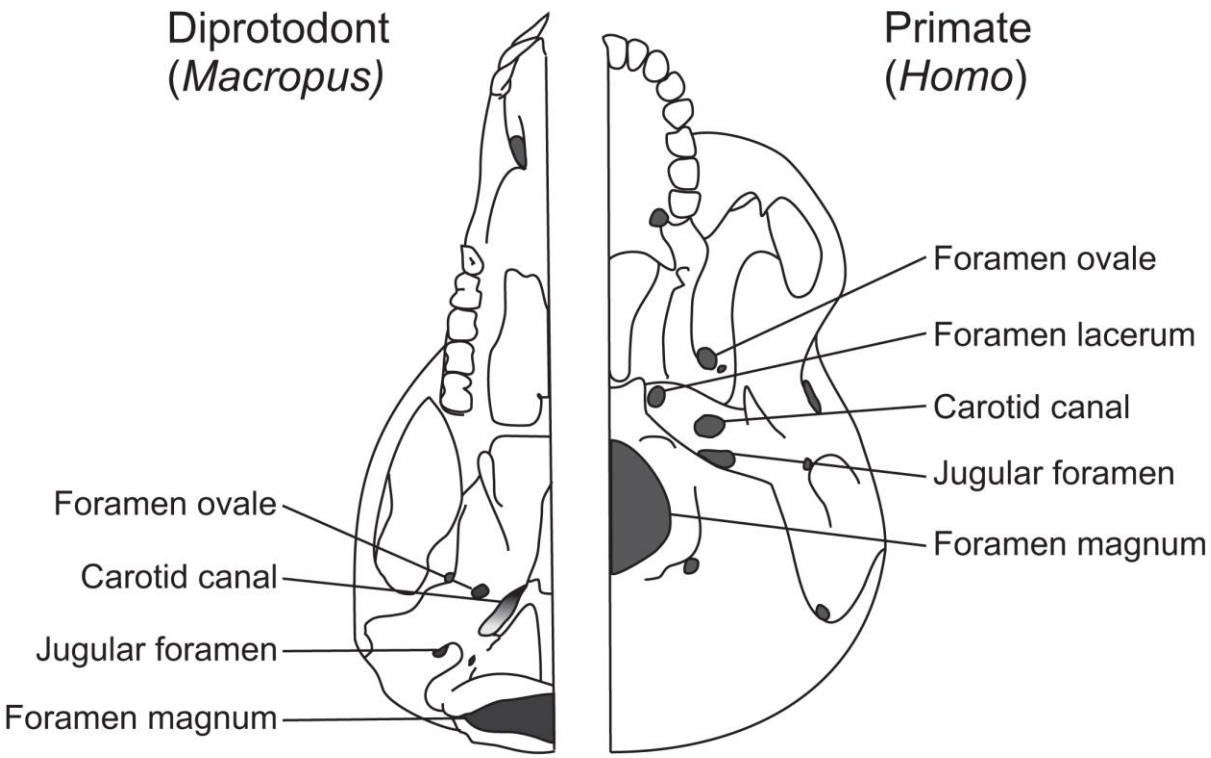

Figure 6. Diagrams of representative skulls of a diprotodont marsupial and a haplorrhine primate, showing the locations of major foramina. The radius of the external opening of the carotid canal is the focus of this study and is easily measured from a ventral view. The carotid canal of the diprotodont enters obliquely and is best viewed from a posterior-ventral-lateral perspective. Note the foramen lacerum of the primate skull, which is plugged with cartilage on the ventral surface, but transmits the carotid artery from the carotid canal into the brain case in life.

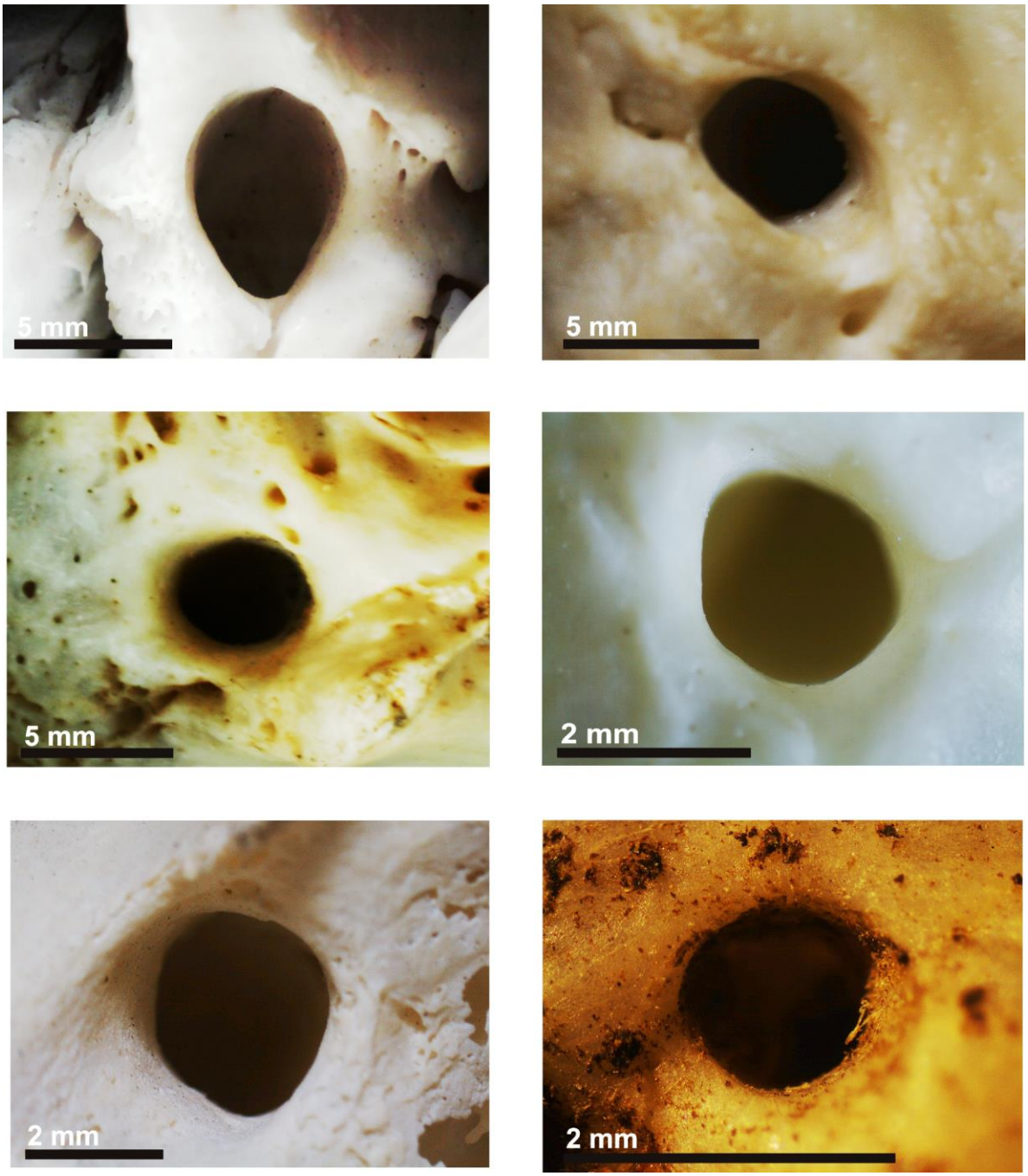

Figure 7. Examples of internal carotid foramina of Haplorrhini. a) *Homo sapiens* (V_{br} = 1186 ml) b) *Pan troglodytes* (V_{br} = 475 ml) c) *Gorilla gorilla* (V_{br} = 461 ml) d) *Hylobates lar* (V_{br} = 103 ml) e) *Papio hamadryas* (V_{br} = 156.5 ml) f) *Saimiri sciureus* (V_{br} = 20 ml).